Yttrium-90-DOTA-Peptide-Chimeric L6 Radioimmunoconjugate: Efficacy and Toxicity in Mice Bearing p53 Mutant Human Breast Cancer Xenografts

Sally J. DeNardo, David L. Kukis, Laird A. Miers, Michelle D. Winthrop, Linda A. Kroger, Qansy Salako, Sui Shen, Kathleen R. Lamborn, Paul H. Gumerlock, Claude F. Meares and Gerald L. DeNardo

Section of Radiodiagnosis and Therapy, Department of Internal Medicine, University of California Davis Medical Center, Sacramento; Brain Tumor Research Center, University of California San Francisco, San Francisco; and Department of Chemistry, University of California Davis, Davis, California

The novel radioimmunoconjugate, ^{90}Y-DOTA-peptide-chimeric L6 (ChL6), was designed to reduce radiation to critical normal tissues with an exceptionally stable ^{90}Y chelate moiety and a biodegradable linker. Human breast cancer tumors (HBT 3477) in mice were treated with ^{90}Y-DOTA-peptide-ChL6 to examine the effects of increasing dose on the therapeutic efficacy and toxicity of this new agent. **Methods:** Groups of athymic mice bearing HBT 3477 xenografts received 4.1- to 14.1-MBq doses of ^{90}Y-DOTA-peptide-ChL6 intravenously. The lethal dose $(LD)_{50/30}$, general well-being (weight loss), hematotoxicity and therapeutic efficacy were studied. **Results:** The $LD_{50/30}$ was 12.8 MBq, which corresponded to doses of 17.9 and 50.9 Gy to the total body and tumor (200 mm^3), respectively. Deaths were associated with hematotoxicity; no deaths occurred at doses of 9.6 MBq or less. At sublethal doses, the rate of tumor response (cures + complete responses + partial responses) increased with increasing dose: 4.1 MBq, 27%; 5.9 MBq, 41%; 8.5 MBq, 69%; and 9.6 MBq, 79% (maximum tolerated dose, MTD). In mice receiving doses of 4.1–9.6 MBq, 6 of 74 (8%) of tumors were cured. Increasing the ^{90}Y dose led to smaller tumor size at nadir and longer tumor regrowth delay but no increase in cure. Although the HBT 3477 *p53* gene was found to be mutant resulting in p53 protein not binding DNA breaks, tumors at MTD demonstrated evidence of apoptosis. **Conclusion:** In the human breast cancer athymic mouse model, ^{90}Y-DOTA-peptide-ChL6 had a high therapeutic index and $LD_{50/30}$ leading to a 79% response rate at the MTD. The evidence of apoptosis as a mechanism for this tumor response in p53 mutant breast cancer warrants further studies because these observations are relevant to the treatment of lethal breast cancer.

Key Words: yttrium-90; breast carcinoma; radioimmunotherapy; apoptosis

J Nucl Med 1998; 39:842–849

Systemic tumor-targeted radiotherapy could provide an important addition to multimodality therapy for incurable metastatic breast cancer based on the potential of this modality to deliver radiation therapy to metastatic cells throughout the body while maintaining a high therapeutic index. We have previously treated breast cancer patients with radioimmunotherapy (RIT) using the human-mouse chimeric monoclonal antibody (MAb), chimeric L6 (ChL6), radiolabeled with ^{131}I, achieving clinically relevant but temporary tumor responses (*1,2*). Yttrium-90 [β e_{max} = 2.3 Mev (100%)], however, provides more effective radionuclide characteristics than ^{131}I [β e_{max} = 0.81 MeV (1%), 0.61 MeV (86%) and 0.34 MeV (13%)] for treatment of solid cancers by providing a more homogeneous dose to the tumor. We performed this study to examine the effects of increasing the ^{90}Y dose on therapeutic efficacy and toxicity, when delivered by a novel biodegradable immunoconjugate, to aggressive human breast cancer tumors implanted in mice.

The radiotherapeutic agent ^{90}Y-DOTA-peptide-ChL6 was designed to minimize the radiation dose to critical normal tissues and optimize the therapeutic index in the treatment of breast cancer. A disadvantage to the use of radiometals in chelate-tagged MAbs for RIT has been the accumulation of radioactivity in nontarget organs, particularly the liver (*3–6*). The linker in ^{90}Y-DOTA-peptide-ChL6 has been shown to be susceptible in vitro to endopeptidase activity, specifically, cathepsin B (*7*). This susceptibility may allow more rapid metabolism and excretion of ^{90}Y from normal organs. The macrocyclic chelating agent DOTA has been shown to bind ^{90}Y with extraordinary stability (*8,9*), resulting in significantly lower loss of ^{90}Y to bone, as compared to the acyclic chelator DTPA in a comparative in vivo study (*10*).

The pharmacokinetics of ^{90}Y-DOTA-peptide-ChL6 in athymic mice bearing human breast cancer xenografts (HBT 3477) have been examined (*11*). Dosimetry calculated from the pharmacokinetic data suggested that an appreciably higher radiation dose could be delivered to the tumor and a greater therapeutic index could be achieved with ^{90}Y-DOTA-peptide-ChL6, as compared to ^{131}I-ChL6. In this study of ^{90}Y-DOTA-peptide-ChL6, the $LD_{50/30}$, general well-being (weight loss), hematotoxicity, therapeutic efficacy and tumor response were evaluated in athymic mice bearing the same human breast cancer xenografts.

MATERIALS AND METHODS

Antibody

Chimeric L6 (Bristol-Myers Squibb, Seattle, WA), an antibody chimera consisting of the constant region of human IgG_1 and the Fab′ region of murine MAb L6, reacts with a membrane antigen found on human adenocarcinoma cells of the lung, colon, ovary and breast (*12,13*).

Cell Line

HBT 3477 (Bristol-Myers Squibb Pharmaceutical Research Institute, Seattle, WA) is a human breast adenocarcinoma cell line. HBT 3477 tumors are aneuploid, with a DNA index of 1.5, and are negative for estrogen and progesterone receptors by immunohistochemistry. L6 and ChL6 have been shown to be reactive with over 70% of HBT 3477 cells (*2,14*). The *p53* gene in the HBT 3477 cell line had shown normal sequencing in exons 6–8, as described

Received Jul. 2, 1997; accepted Aug. 4, 1997.

For correspondence or reprints contact: Sally J. DeNardo, MD, Molecular Cancer Institute, 1508 Alhambra Boulevard, Suite 3100, Sacramento, CA 95816.

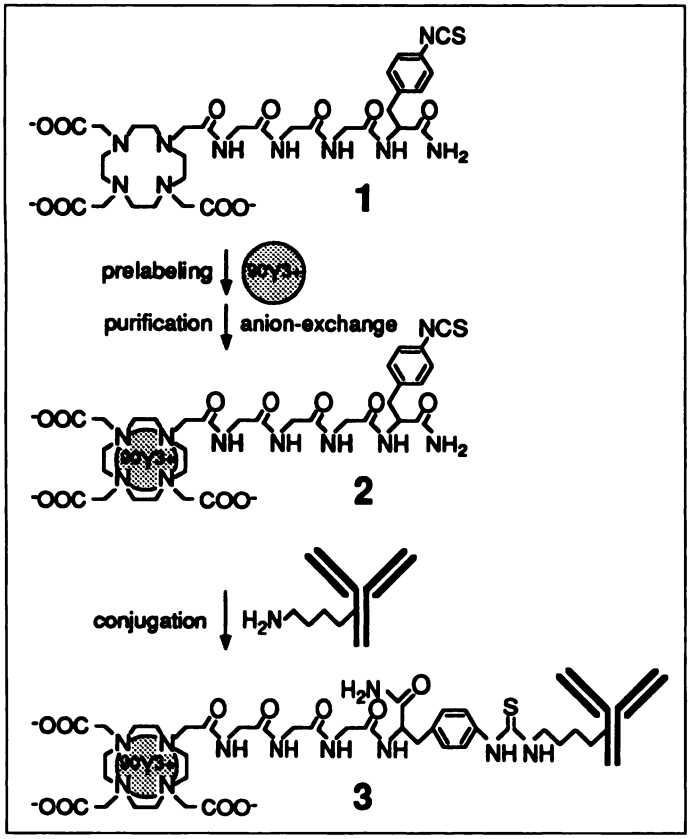

FIGURE 1. Preparation of ^{90}Y-DOTA-peptide-ChL6 by the prelabeling method. The bifunctional chelate, DOTA-peptide-NCS (1), was labeled with ^{90}Y, and then the neutral radiolabeled chelate was purified by anion exchange chromatography to eliminate excess chelating agent and other charged species (i.e., chelates of divalent metal ion contaminants in ^{90}Y). Purified ^{90}Y-DOTA-peptide-NCS (2) was then conjugated to ChL6 MAb to yield ^{90}Y-DOTA-peptide-ChL6 (3), which was purified by centrifuged column filtration to yield final radioimmunoconjugate.

previously (*15,16*); the codon for DNA binding in exon 10 has now been evaluated in the same manner.

Apoptotic Analysis by Poly(ADP-Ribose) Polymerase Cleavage

One tumor sample each was harvested before therapy and 6 hr after ^{90}Y-DOTA-peptide-ChL6 therapy to evaluate poly(ADP-ribose) polymerase (PARP) cleavage. Protein from each sample was separated by SDS-PAGE and transferred to a nitrocellulose membrane. The membrane was incubated with a mouse anti-PARP MAb (PharMingen, San Diego, CA), followed by a secondary antibody and streptavidin-peroxidase. Bands were visualized using chemiluminescence reagents (*17*).

Synthesis of DOTA-Peptide-NCS

The bifunctional chelating agent DOTA-glycylglycylglycyl-L-p-isothiocyanatophenylalanine (DOTA-peptide-NCS) (Fig. 1) was prepared as described previously (*7*). The tetrapeptide linker glycylglycylglycyl-p-nitrophenylalanine was coupled to 1,4,7,10-tetraazacyclododecane-N,N′,N″,N‴-tetraacetic acid (DOTA) via an amide bond followed by conversion of the nitrobenzyl group to an isothiocyanatobenzyl group. DOTA-peptide-NCS was purified by reverse-phase high-performance liquid chromatography (HPLC) and characterized by proton nuclear magnetic resonance spectrometry, fast atom bombardment mass spectrometry and KBr infrared spectroscopy. The ability of DOTA-peptide-NCS to bind metal was confirmed by ^{57}Co-binding assay (*18*).

Preparation of Yttrium-90-DOTA-Peptide-ChL6

Yttrium-90-DOTA-glycylglycylglycyl-L-phenylalanyl-thiourea-ChL6 (^{90}Y-DOTA-peptide-ChL6) was prepared by the prelabeling method described previously (*11,19*) (Fig. 1). Briefly, ^{90}Y (Amersham, Arlington Heights, IL) (0.70 GBq in 0.04 *M* HCl) was dried on a heating block under N_2 (g), then DOTA-peptide-NCS (1.0 μmole in 100 μl of 0.1 *M* tetramethylammonium acetate, pH 5.0) was added and the solution was incubated for 1 hr at 37°C. DTPA was added to a final concentration of 10 m*M* to scavenge unchelated ^{90}Y. The solution was applied to diethylaminoethyl-cellulose anion exchange resin (Sigma Chemical Co., St. Louis, MO) (0.2 ml), which had been converted to acetate form. Purified ^{90}Y-DOTA-peptide-NCS (0.53 GBq) was eluted in water (0.4 ml); the solution was concentrated to 23 μl under vacuum. Chimeric L6 (6.0 mg in 108 μl of 0.1 *M* tetramethylammonium phosphate, pH 8.0) was added, and the pH was adjusted to 9.5 with 2 *M* triethylamine. The conjugation reaction solution was incubated for 1 hr at 37°C, and ^{90}Y-DOTA-peptide-ChL6 (0.16 GBq/6 mg) was isolated and transferred to 0.9% saline/10 m*M* sodium phosphate (pH 7.6) by centrifuged gel filtration (*20,21*). The product yield for the radiolabeling was 23%. A second labeling was performed similarly, yielding 0.94 GBq/10 mg ^{90}Y-DOTA-peptide-ChL6 with a 38% product yield.

Quality Control

Yttrium-90-DOTA-peptide-ChL6 was examined by cellulose acetate electrophoresis (CAE), molecular sieving HPLC and radioimmunoreactive assay (RIA) (*11*). CAE (Gelman Sciences, Inc., Ann Arbor, MI) was performed using 0.05 *M* sodium barbital buffer, pH 8.6. A current of 5 mA per strip was applied. Samples were electrophoresed for 11 and 45 min. At 11 min, free chelates were resolved from immunoconjugates. At 45 min, monomeric immunoconjugates were resolved from aggregated species. HPLC (Beckman 332, Beckman, San Ramon, CA) was performed using a molecular sieving column (Beckman SEC-3000) eluted in 0.1 *M* sodium phosphate/0.1 *M* potassium sulfate/0.025% (w/v) sodium azide (pH 7.1). The flow rate was 1.0 ml/min. Radiolabeled MAbs and conjugates were detected by UV absorbance at 280 nm (Beckman 166 detector) and radioactivity (Beckman 170 detector). Immunoreactivity of ^{90}Y-DOTA-peptide-ChL6 was assessed by cell binding RIA using the HBT 3477 adenocarcinoma cell line as described previously (*11,22*). Iodine-125-ChL6 was assayed in parallel as a standard. All RIA samples were counted in a well counter (Pharmacia LKB 1282, Pharmacia, Piscataway, NJ).

Greater than 99% of ^{90}Y was associated with immunoconjugate, and less than 7% of immunoconjugate was in aggregated form by CAE and HPLC. The absolute immunoreactive binding in the live cell assays was 73% or more and, relative to the ^{125}I-ChL6 standard, 90% or more.

Mouse Studies

Female athymic mice (Harlan Sprague-Dawley, Frederick, MD), 7–9 wk of age, were maintained according to University of California animal care guidelines on a normal diet ad libitum and under pathogen-free conditions. Five mice were housed per cage. To minimize ambient radiation dose, bedding was changed daily for 1 wk after treatment with ^{90}Y-DOTA-peptide-ChL6 and twice weekly thereafter.

HBT 3477 cells were grown in Iscove's medium and harvested in the logarithmic phase, and 2.5–5.0 × 10^6 cells were injected subcutaneously into both sides of the abdomen of each mouse. Three weeks after implantation, when the range of tumor volumes was 28–203 mm^3, the mice received an intravenous injection in the tail vein of ^{90}Y-DOTA-peptide-ChL6 at one of six dose levels in groups of 9–11 animals per dose level. The doses administered were 4.1, 5.9, 8.5, 9.6, 12.2 and 14.1 MBq (110, 160, 230, 260, 330

and 380 μCi). The largest protein dose required to administer a desired activity of ^{90}Y was 315 μg of ChL6. Unmodified ChL6 was added to all other doses of radioimmunoconjugate so that each mouse received an equal protein dose of 315 μg of MAb (*23*). An ionization chamber dose calibrator (Capintec CRC-12, Capintec, Inc., Pittsburgh, PA), calibrated for containers and volumes using ^{90}Y standards, was used to measure ^{90}Y-DOTA-peptide-ChL6 doses. To calculate the activity of ^{90}Y, samples were measured at a dose calibrator setting of 048, and the readings were multiplied by 10, in accordance with current National Institute of Standards and Technology convention (*24*). Control groups of 10 and 8 tumored mice received no treatment and 315 μg of unlabeled ChL6, respectively. Survival was monitored daily; mouse weight and tumor size were measured 2–3 times per week for 12 wk postinjection or until death.

Tumors were measured in three orthogonal diameters with a caliper, and tumor volume, V, was calculated by the formula for hemiellipsoids:

$$V = (4/3)(\pi)(d_1/2)(d_2/2)(d_3/2). \quad \text{Eq. 1}$$

Red blood cell (RBC), platelet and white blood cell (WBC) counts were measured 2–3 times per week for 12 wk postinjection as follows. Blood samples were collected from tail veins with 2 μl of microcapillary pipets, and samples from mice within a dose group were pooled. The pooled samples were diluted 1:200 in 0.9% saline/10 m*M* sodium phosphate (pH 7.6) for RBC counts; 1:100 in 1% (w/v) ammonium oxalate for platelet counts; and 1:20 in 3% (w/v) acetic acid for WBC counts.

Tumor volumes, mouse weights and blood counts in all mice alive on the day of measurement were used to calculate the mean values for a dose group on that day.

Analysis of Tumoricidal Effect

Initial tumor volumes were measured 1 day before treatment with ^{90}Y-DOTA-peptide-ChL6. In the calculation of mean tumor size, tumors that had completely regressed were considered tumors with a volume of 0. Doubling time of tumors in control groups was calculated by regression of log mean tumor size versus time for 84 days.

A period of tumor regression was defined for each dose group as follows. The period began on the median day on which the tumors in a dose group reached an initial peak in volume and ended on the median day on which the tumors subsequently reached a nadir in volume before regrowing. A rate of regression was calculated for every tumor by monoexponential curve fitting of tumor volume data over the period of tumor regression. Tumors that grew during the period had a negative rate of regression. A mean rate of tumor regression was calculated for each dose group.

Tumor regrowth delay is a conventional method used to evaluate the effect of a therapeutic regimen on tumor size over an extended period of time (*25–27*). The tumor regrowth delay for a given dose was calculated as the number of days required for the mean tumor volume of the dose group to reach two times the mean initial tumor volume minus the number of days required for the mean tumor volume in the untreated control group to reach two times the mean initial tumor volume.

For every tumor that reached a nadir, its volume at nadir relative to its initial volume was calculated to evaluate the possible relationship between ^{90}Y dose and logarithmic cell kill.

Tumor responses were categorized as follows: cure (C), tumor disappeared and did not recur by the end of the 12-wk study; complete regression (CR), tumor disappeared, but later reoccurred; and partial regression (PR), tumor decreased by 50% or more in volume but did not disappear.

TABLE 1
Biodistribution of Yttrium-90-DOTA-Peptide-Chimeric L6 in the Athymic Mouse HBT Model*

	%ID/g†		
	Day 1	Day 3	Day 5
Tumor	17.5 ± 8.0	18.0 ± 8.0	13.8 ± 5.2
Liver	6.3 ± 1.4	5.5 ± 1.4	5.8 ± 1.9
Lung	8.4 ± 2.2	5.9 ± 1.0	4.9 ± 1.0
Kidney	5.6 ± 0.3	4.6 ± 0.7	3.6 ± 0.9
Blood‡	51 ± 7	38 ± 4	30 ± 2
Total body‡	88 ± 10	58 ± 11	26 ± 18

*DeNardo et al. (*11*).
†Mean ± s.d.
‡Values are %ID.

Mortality Calculations

Deaths within 30 days of treatment were attributed to the toxic effects of ^{90}Y-DOTA-peptide-ChL6. Cumulative mortality curves were constructed and logistic regression analysis (SAS system software, SAS Institute, Inc., Cary, NC) was used to calculate an estimate of the dose lethal to 50% of mice within 30 days ($LD_{50/30}$). A 95% confidence interval was calculated by Fieller's method (*28*). To corroborate the results, an estimate of the $LD_{50/30}$ dose was also calculated by the Reed-Meunch method (*10,29*).

Dosimetry Calculations

With an X_{90} distance of 0.52 cm in water (*30*), the beta particles of ^{90}Y should be treated as penetrating radiation in a small object such as a mouse. For targets (liver, lungs, kidneys, tumor and marrow) considered here, the total dose to target, D_t, was estimated by:

$$D_t = D_{t\leftarrow t} + \sum D_t \leftarrow k + D_{t\leftarrow RB}, \quad \text{Eq. 2}$$

where $D_{t\leftarrow t}$ is the target-to-target dose, $D_{t\leftarrow k}$ is the nontarget-to-target dose and $D_{t\leftarrow RB}$ is the dose to target contributed by the remainder of the body defined as the total body minus liver, kidneys and lungs (*10*). The absorbed fraction for each organ from Hui et al. (*31*) was used. For marrow as target organ, $D_{t\leftarrow t}$ was contributed from the blood, and a specific activity of 0.25 for marrow in blood was used (*32*). Whole-body and blood clearances were performed on the mice in this study and were unchanged from those previously reported in the detailed biodistribution studies (*11*). Therefore, organ and tumor uptake and clearance from the previously performed biodistribution studies were used to calculate projected organ doses. Dosimetry calculations were performed as described previously (*16,33*).

The cumulated activity of tumor was estimated by integrating the time-activity curve, based on the results of previous studies of the biodistribution of ^{90}Y-DOTA-peptide-ChL6 in HBT-tumored mice (Table 1) (*11*). For tumor as the target, the self-absorbed fraction for tumors of 30 mm^3, 100 mm^3 and 200 mm^3 in volume, representing the range of volume in the current study, was used to calculate dose to tumors (*34*).

Statistical Analysis

Sets of data grouped according to dose of ^{90}Y-DOTA-peptide-ChL6 were compared by the nonparametric Jonkheere-Terpstra exact test (*35*) (StatXact 3, Cytel Corp., Cambridge, MA). The Jonkheere–Terpstra exact test was designed for multiple-group comparisons in which the property examined might be expected to be ordered across groups (i.e., the period of tumor regression may increase with increasing dose). The test generates a one-sided p value that indicates whether the observed increase (decrease) with increasing dose may be due to chance.

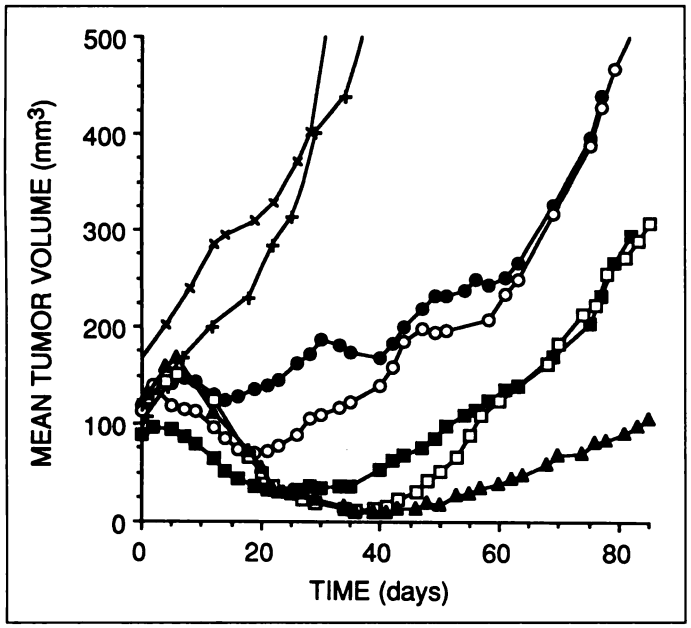

FIGURE 2. Mean volume of HBT tumors in mice receiving ^{90}Y-DOTA-peptide-ChL6 at doses of 4.1 (●), 5.9 (○), 8.5 (■), 9.6 (□) and 12.2 (▲) MBq. Tumors regressed in all treatment groups, reaching a nadir at 14–58 days postinjection. Higher doses were associated with more prolonged tumor regression. Tumors in untreated mice (+) and mice receiving unlabeled ChL6 (×) grew without interruption.

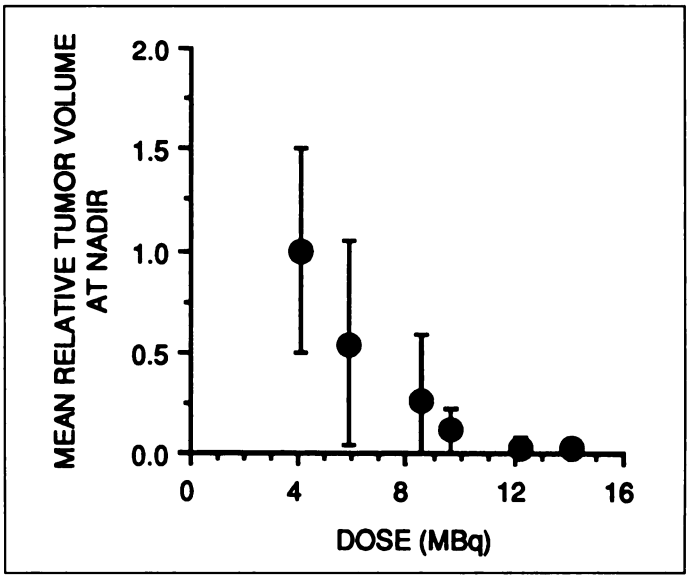

FIGURE 3. Relative size of HBT tumors at nadir indexed against initial tumor size, compared to dose of ^{90}Y-DOTA-peptide-ChL6. Higher ^{90}Y dose was associated with greater tumor regression. ●, mean relative size of 14 or more tumors at nadir, except at 14.1 MBq (two tumors); bars, s.d.

Comparisons of response among treatment groups were done using the Cochran-Mantel-Haensel method (*36*). The test generates a p value that indicates whether the observed differences in response among treatment groups may be due to chance. A ranking based on the quality of the response was assigned ordered as C, CR, PR and no response. To minimize the possibility of declaring the therapy effective when it was not, statistical testing was done in the following order. First, a test was done to determine whether chance alone could explain the observed differences among all groups. Second, a test was done to see if chance alone could explain any differences among the control groups. Third, comparison was made among the groups receiving ^{90}Y-DOTA-peptide-ChL6 therapy.

RESULTS

p53 Mutational Status

Sequencing the exon 10 region of the *p53* gene from the HBT 3477 cell line used in this study demonstrated a mutation creating a "stop" codon at codon 342 for the carboxyl-terminal region of p53 protein, precluding production of normal p53 protein. No normal sequence for this region was detected.

Tumoricidal Effect

The following observations are restricted to doses of 12.2 MBq or less of ^{90}Y-DOTA-peptide-ChL6 because 14.1 MBq was too toxic to yield meaningful efficacy data.

The mean tumor volume increased slightly immediately after treatment, decreased to a nadir and then increased again; comparatively, tumors in the control groups grew without interruption, with doubling times of 19 and 20 days for mice receiving no treatment and unlabeled ChL6, respectively (Fig. 2). The median day at which tumors in the 4.1-MBq dose group reached an initial peak in size was 7 days after treatment; the median day at which they reached a nadir was 14 days after treatment. During this period, the tumors shrank at a rate (mean ± s.d.) of 2.8% ± 4.2% per day. The periods of regression and rates of tumor shrinkage for the other dose groups were: 5.9 MBq, days 2–19, 5.2% ± 5.9% per day; 8.5 MBq, days 5–22, 11.8% ± 8.8%; 9.6 MBq, days 4–36, 8.3% ± 2.5%; and 12.2 MBq, days 4–35, 9.3% ± 4.0%. Although there were no statistically significant differences in the rates of tumor shrinkage among dose groups, higher dose was associated with a longer period of regression (Jonkheere-Terpstra exact test, $p < 0.001$). The mean tumor volume at nadir decreased with increasing dose (Jonkheere-Terpstra exact test, $p < 0.001$) (Fig. 3), showing that a higher dose resulted in greater cell kill.

The time required for the mean tumor volume to increase to two times the initial volume was 6 and 21 days for the control groups receiving no treatment and unmodified ChL6, respectively, and 47, 54, 69 and 74 days for the 4.1-, 5.9-, 8.5- and 9.6-MBq dose groups, respectively. In the 12.2-MBq dose group, the mean tumor volume never reached two times the initial volume over the 84-day study. The regrowth delay was calculated to be 41, 48, 63, 68 and greater than 78 days for the 4.1, 5.9-, 8.5-, 9.6- and 12.2-MBq dose groups, respectively.

The response of tumors to treatment with ^{90}Y-DOTA-peptide-ChL6 is summarized in Table 2. By Cochran-Mantel-Haensel analysis, differences among all groups were found to be significant ($p < 0.01$). The untreated group and the group treated with unmodified ChL6 were not different from one another ($p = 0.5$). The response of the groups treated with ^{90}Y-DOTA-peptide-ChL6 differed significantly from the control groups ($p = 0.02$). Among the groups receiving ^{90}Y-DOTA-peptide-ChL6 therapy at sublethal doses, the percentage of tumors achieving a response (Cs, CRs or PRs) increased with increasing dose, reaching 79% at 9.6 MBq. The dose response effect was significant ($p < 0.01$).

Poly(ADP-Ribose) Polymerase Analysis of Apoptosis After ^{90}Y-DOTA-Peptide-Chimeric L6

Cleavage of PARP from its intact size of 116 kDa to a 85-kDa fragment, characteristic of cells undergoing apoptosis, was detected 6 hr after treatment of the HBT 3477 xenografts with 260 μCi of ^{90}Y-DOTA-peptide-ChL6 (Fig. 4).

Mortality

Of mice treated with ^{90}Y-DOTA-peptide-ChL6, deaths within 30 days occurred only at the two highest doses: 12.2 MBq (3 of 10 mice died) and 14.1 MBq (8 of 9 mice died) (Fig. 5). The median time of death was 18.5 days (range 15–22 days).

TABLE 2
Response of HBT Human Breast Cancer Xenografts to Yttrium-90-DOTA-Peptide-Chimeric L6 Treatment

Treatment	No. of tumors/ no. of mice	Initial tumor volume* (mm^3)	No. of Cs	No. of CRs	No. of PRs	Response rate† (%)	Deaths <30 days (%)
Control							
No treatment	17/10	82 (28–146)	0	0	3	18	10
ChL6, 315 μg	16/8	160 (55–328)	2	0	0	13	13
Treatment							
^{90}Y-ChL6, 4.1 MBq	22/11	108 (50–156)	2	0	4	27	0
^{90}Y-ChL6, 5.9 MBq	17/9	108 (42–182)	1	0	6	41	0
^{90}Y-ChL6, 8.5 MBq	16/9	80 (28–140)	3	1	7	69	0
^{90}Y-ChL6, 9.6 MBq	19/10	100 (44–196)	0	3	12	79	0
^{90}Y-ChL6, 12.2 MBq	20/10	107 (50–203)	4	6	4	70	30
^{90}Y-ChL6, 14.1 MBq	18/9	87 (31–140)	1	0	1	11‡	89

*Values are means (ranges).
†Response = Cs + CRs + PRs.
‡Reflects the large number of deaths in this group.
C = cure; CR = complete regression; PR = partial regression.

The temporal occurrence of death was consistent with radiation myelotoxicity, which was supported by the RBC and WBC counts. By logistic regression, the lethal dose $(LD)_{50/30}$ was estimated to be 12.8 MBq (95% confidence interval = 11.8–13.9). Comparatively, the $LD_{50/30}$ was estimated to be 12.9 MBq by the Reed–Meunch method.

Weight Loss

The surviving mouse that received 14.1 MBq of ^{90}Y-DOTA-peptide-ChL6 exhibited severe and prolonged weight loss (Fig. 6), reaching a nadir at day 18 with the loss of 34% of initial body weight. Mice receiving 9.6 and 12.2 MBq lost 15% and 13% of their initial body weight, respectively, and began regaining weight by day 7. The weight loss of lower dose groups, if any, was very mild and transient.

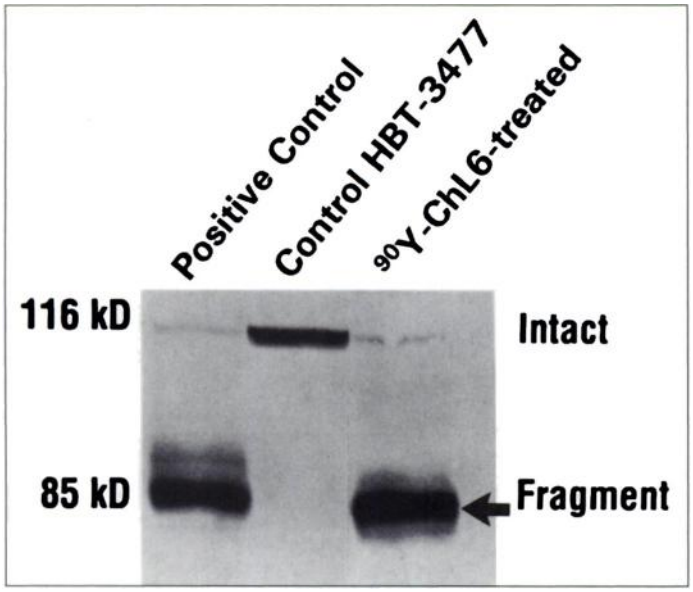

FIGURE 4. Apoptosis in the HBT 3477 after ^{90}Y-DOTA-peptide-ChL6 treatment is evidenced by cleavage of PARP from the 116-kDa form to its characteristic apoptotic fragment (85 kDa) 6 hr post-therapy. Lane 1, positive control prostate cancer (LNCaP)-treated cells (note the PARP fragment); Lane 2, untreated control HBT 3477 xenografts; Lane 3, HBT-treated tumor 6 hr post-therapy at MTD, demonstrating the specific PARP fragment cleaved during apoptosis.

Myelotoxicity

The evidence of hematotoxicity was consistent for all groups (Fig. 7). WBC and platelet counts declined 1–4 days postinjection, and RBC counts declined later and to a lesser extent. Higher ^{90}Y doses were associated with more severe and prolonged suppression of counts.

Dosimetry

Blood and whole-body clearances were statistically unchanged from those previously published as part of a biodistribution study (*11*). Target-to-target and body-to-target doses received by major organs and tumor were estimated (Table 3). In the mouse, the relative contribution of ^{90}Y radiation dose from body to normal organs was large, constituting 15%, 43%, 68% and 71% of the total dose to liver, kidney, marrow and lungs, respectively. Comparatively, body-to-tumor dose consti-

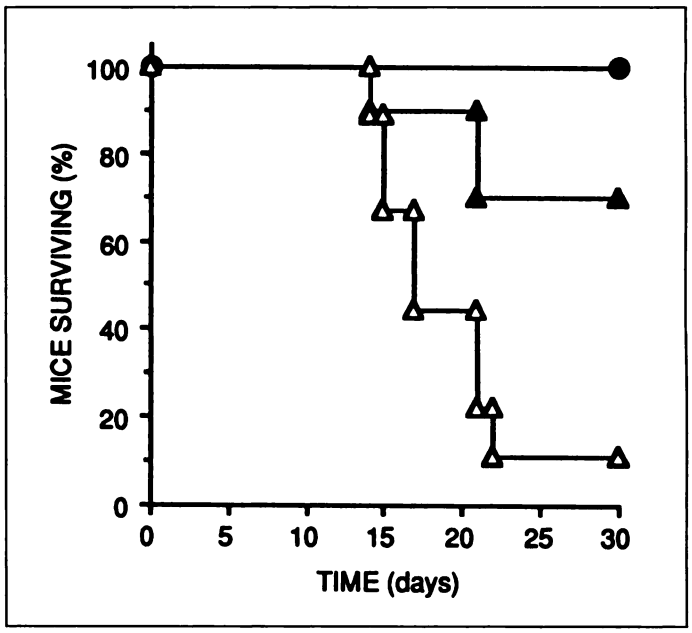

FIGURE 5. Survival of HBT-tumored mice after treatment with ^{90}Y-DOTA-peptide-ChL6. No treated mouse receiving 9.6 MBq or less (●) died within 30 days. Mortalities occurred at the 12.2-MBq (▲) and 14.1-MBq (△) dose levels. The $LD_{50/30}$ was estimated to be 12.8 MBq by logistic regression.

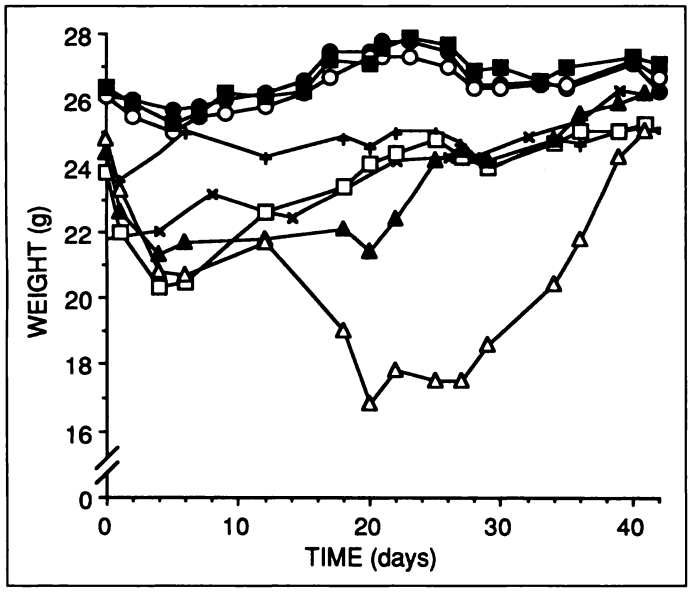

FIGURE 6. Weights of mice receiving no treatment (+), unlabeled ChL6 (×) and ^{90}Y-DOTA-peptide-ChL6 in doses of 4.1 (●), 5.9 (○), 8.5 (■), 9.6 (□), 12.2 (▲) and 14.1 (△) MBq. Higher doses were associated with more severe and prolonged weight loss. Weights were normal within 40 days after therapy. Data points, mean weights of 9 to 11 mice, except at 12.2 MBq (10 mice decreasing to 7) and 14.2 MBq (9 mice decreasing to 1).

tuted 12%, 15% and 20% of the total dose to tumors of volumes 200, 100 and 30 mm^3, respectively.

The $LD_{50/30}$ dose of ^{90}Y-DOTA-peptide-ChL6 corresponded to a total-body radiation dose of 17.9 Gy. Comparatively, the $LD_{50/30}$ for an acute body radiation dose to Balb/c mice from external beam radiation has been reported to be 5.5–7.5 Gy (*37,38*).

DISCUSSION

Our study was designed to evaluate a novel ^{90}Y immunoconjugate as a therapeutic modality for aggressive breast cancer. With an exceptionally stable ^{90}Y chelate moiety and a unique biodegradable linker to reduce hepatic accumulation of radioactivity, ^{90}Y-DOTA-peptide-ChL6 was designed to minimize the radiation dose to normal tissues.

The $LD_{50/30}$ was 12.8 MBq, which is relatively high when compared to other ^{90}Y radioimmunoconjugates in mice (*39,40*). The enhanced tolerance of ^{90}Y when given as ^{90}Y-DOTA-peptide-ChL6 is most likely secondary to the stability of ^{90}Y in the DOTA chelate, resulting in little or no loss of ^{90}Y to bone (*8,9*). It is anticipated that the enhanced tolerance would be more pronounced in humans. In the mouse model, the beta energy from ^{90}Y is sufficiently great so as to provide significant additive radiation to critical normal tissues, such as marrow, because of their proximity to tissues with higher uptake (liver, spleen and bladder), whereas in humans, this is not the case.

The radiation dose to the bodies of mice was estimated as 17.9 Gy at the $LD_{50/30}$ dose, appreciably higher than the external beam acute total body LD_{50} previously published for athymic mice (*37,38*). However, it has been demonstrated that, at comparable total doses, lower dose rate radiation is associated with less toxicity to normal tissues (*41*).

The ChL6 MAb used for the radioimmunoconjugate has been shown to be reactive with the majority of HBT cells used for the subcutaneous tumors in the mice (*2,14*). In previous studies of the biodistribution of ^{90}Y-DOTA-peptide-ChL6 in athymic mice bearing HBT tumors, uptake of 18% of the injected dose per g of tumor was observed. In our study, at the time of therapy, the mean mass of the treated tumors was approximately

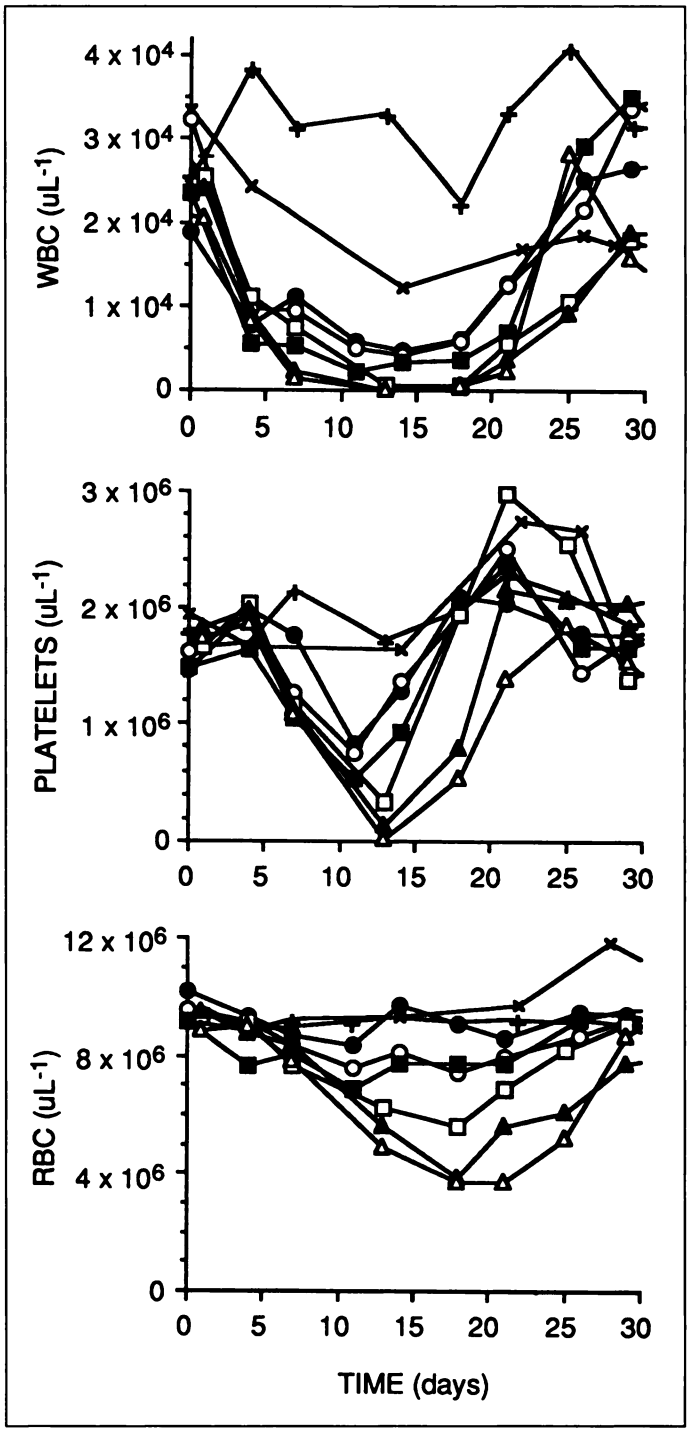

FIGURE 7. White blood cell, platelet and RBC counts in mice receiving no treatment (+), unlabeled ChL6 (×) and ^{90}Y-DOTA-peptide-ChL6 in doses of 4.1 (●), 5.9 (○), 8.5 (■), 9.6 (□), 12.2 (▲) and 14.1 (△) MBq. Higher doses were associated with greater suppression of counts. Blood counts returned to normal within 30 days after therapy. Data points, pooled samples from 9 to 11 mice, except at 12.2 MBq (10 mice decreasing to 7) and 14.1 MBq (9 mice decreasing to 1).

100 mg (range 28–203 mg). Among tumors in this size range, assuming the same uptake of ^{90}Y-DOTA-peptide-ChL6 per g, the radiation dose per unit activity injected increased with increasing tumor size (Table 3). On the other hand, previous studies have demonstrated that smaller tumors usually have substantially greater uptake, which may somewhat negate the loss of efficiency (*42,43*).

The highest nonlethal dose of ^{90}Y-DOTA-peptide-ChL6, 9.6 MBq was considered the maximum tolerated dose (MTD). At

TABLE 3
Radiation Doses (Gy) to Mice from Yttrium-90-DOTA-Peptide-ChL6 Therapy

	Radiation dose per MBq		Total radiation dose	
	Target-to-target	Nontarget-to-target	At MTD, 9.6 MBq	At $LD_{50/30}$, 12.8 Mbq
Whole body	1.4	na	13.4	17.9
Marrow	0.40	0.85	12.0	16.0
Tumor				
30 mm^3	2.2	0.54	26.3	35.1
100 mm^3	2.9	0.51	32.7	43.6
200 mm^3	3.5	0.48	38.2	50.9
Liver	1.8	0.32	20.4	27.1
Lung	0.76	1.8	24.6	32.8
Kidney	0.88	0.67	14.9	19.8

na = not applicable; MTD = maximum tolerated dose; LD = lethal dose.

sublethal doses, the rate of responding tumors increased with the injected dose ($p < 0.001$). At MTD, the tumor response rate (Cs + CRs + PRs) was 79%, a high response rate in an aggressive breast cancer model. However, only 6 of 74 tumors were cured overall.

The normal growth of HBT tumors in athymic mice showed a doubling time of 19 days. Complete regression for at least a month of tumors of the size used in our study suggests that approximately 10^8 tumor cells were reduced to approximately 10^5. All tumor cells should have received comparable radiation doses because ^{90}Y has been demonstrated both by autoradiography and by dosimetric calculations to deliver relatively homogeneous radiation to tumors of this size (*11*). Thus, relative radioresistance of some tumor cells is suggested and could be related to a substantial tumor population in G_0 of the cell cycle, the expression of genes enhancing cell cycle radioresistance and subpopulations harboring relevant genetic mutants (*44,45*). Recent studies have demonstrated a key role of the *p53* gene (and its transcribed protein) in tumor response to radiation (*46–48*). Therefore, the *p53* gene in HBT 3477 tumors was evaluated. The presence of only mutant codon 342 in the *p53* gene, which produces a short p53 protein that cannot bind DNA breaks, may partially explain the radioresistance of this tumor (*49*). The abundance of specific PARP 85-kDa fragments in MTD-treated tumor compared to minimal levels in untreated tumors suggests that programmed cell death (apoptosis) is a significant mechanism of cell death from this therapy despite the mutant p53 (Fig. 3) (*17,50*). Because increasing evidence has demonstrated p53 mutations in aggressive breast cancer, therapy of this breast cancer model is considered particularly relevant to the therapy of patients (*51,52*). The response of the aggressive HBT tumor to single modality therapy with ^{90}Y-DOTA-peptide-ChL6 has been investigated as a prospective component of multimodality therapy for breast cancer. Further molecular studies of therapeutic response to RIT in this and other human tumor models may lead to the selection of effective combination therapy for aggressive breast cancer.

CONCLUSION

Radioimmunotherapy represents a potentially effective method of delivering systemic radiation therapy to metastatic breast cancer. In a human breast cancer athymic mouse model that exhibits many characteristics of lethal breast cancers in humans, ^{90}Y-DOTA-peptide-ChL6 had a high therapeutic index and $LD_{50/30}$ with a 79% response rate at the MTD. Responses in most instances were followed by a recurrence of the tumor. The promising results warrant further studies of methods, e.g., sequential therapy and multimodality therapy, to eradicate the remaining tumor cell population, so that cure becomes more common.

ACKNOWLEDGMENTS

This research was supported by National Cancer Institute Grants CA47829 and CA16861 and the Department of Energy Grant DE-FG03-84ER60233 and Society of Nuclear Medicine Education and Research Foundation Student Fellowships to Michelle D. Winthrop, PhD, 1994 and 1995.

REFERENCES

1. DeNardo SJ, O'Grady LF, Richman CM, DeNardo GL. Overview of radioimmunotherapy in advanced breast cancer using I-131 chimeric L6. In: Ceriani RL, ed. *Antigen and antibody molecular engineering in breast cancer diagnosis and treatment.* New York: Plenum Press; 1994:203–211.
2. DeNardo SJ, Mirick GR, Kroger LA, et al. The biologic window for chimeric L6 radioimmunotherapy. *Cancer* 1994;73(suppl):1023–1032.
3. Vriesendorp HM, Quadri SM, Andersson BS, Dicke KA. Hematologic side effects of radiolabeled immunoglobulin therapy. *Exp Hematol* 1996;24:1183–1190.
4. Wong JY, Williams LE, Yamauchi DM, et al. Initial experience evaluating yttrium-90-radiolabeled anti-carcinoembryonic antigen chimeric T84.66 in a Phase I radioimmunotherapy trial. *Cancer Res* 1995;55(suppl):5929s–5934s.
5. Wilder RB, DeNardo GL, DeNardo SJ. Radioimmunotherapy: recent results and future directions. *J Clin Oncol* 1996;14:1383–1400.
6. Arano Y, Mukai T, Akizawa H, et al. Radiolabeled metabolites of proteins play a critical role in radioactivity elimination from the liver. *Nucl Med Biol* 1995;22:555–564.
7. Li M, Meares CF. Synthesis, metal chelate stability studies, and enzyme digestion of a peptide-linked DOTA derivative and its corresponding radiolabeled immunoconjugates. *Bioconjug Chem* 1993;4:275–283.
8. Moi MK, Meares CF, DeNardo SJ. The peptide way to macrocyclic bifunctional chelating agents: synthesis of 2-(p-nitrobenzyl)-1,4,7,10-tetraazacyclododecane-N,N′,N″,N‴-tetraacetic acid and study of its yttrium (III) complex. *J Am Chem Soc* 1988;110:6266–6267.
9. Deshpande SV, DeNardo SJ, Kukis DL, et al. Yttrium-90-labeled monoclonal antibody for therapy: labeling by a new macrocyclic bifunctional chelating agent. *J Nucl Med* 1989;30:473–479.
10. DeNardo GL, Kroger LA, DeNardo SJ, et al. Comparative toxicity studies of yttrium-90 MX-DTPA and 2-IT-BAD conjugated monoclonal antibody (BrE-3). *Cancer* 1994;73(suppl):1012–1022.
11. DeNardo SJ, Zhong G-R, Salako Q, Li M, DeNardo GL, Meares CF. Pharmacokinetics of chimeric L6 conjugated to indium-111- and yttrium-90-DOTA-peptide in tumor-bearing mice. *J Nucl Med* 1995;36:829–836.
12. Fell HP, Gayle MA, Yelton D, et al. Chimeric L6 anti-tumor antibody: genomic construction, expression, and characterization of the antigen binding site. *J Biol Chem* 1992;267:15552–15558.
13. Liu AY, Robinson RR, Hellström KE, Murray ED, Chang CP, Hellström I. Chimeric mouse-human IgG1 antibody that can mediate lysis of cancer cells. *Proc Natl Acad Sci USA* 1987;84:3439–3443.
14. Adams GP, DeNardo SJ, Amin A, et al. Comparison of the pharmacokinetics in mice and the biological activity of murine L6 and human-mouse chimeric ChL6 antibody. *Antibodies Immunoconj Radiopharm* 1992;5:81–95.
15. Chi, SG, deVere White RW, Meyers FJ, Siders DB, Lee F, and Gumerlock PH. p53 in prostate cancer: frequent expressed transition mutations. *J Natl Cancer Inst* 1994;86:926–933.
16. DeNardo SJ, Gumerlock PH, Winthrop MD, et al. Yttrium-90 chimeric L6 therapy of human breast cancer in nude mice and apoptosis related mRNA expression. *Cancer Res* 1995;55:5837–5841.
17. Tewari M, Quan LT, O'Rourke D, et al. Yama/CPP32B, a mammalian homolog of CED-3, is a CrmA-inhibitable protease that cleaves the death substrate poly(ADP-ribose) polymerase. *Cell* 1995;81:801–809.
18. Goodwin DA, Meares CF, Watanabe N, et al. Pharmacokinetics of pretargeted monoclonal antibody 2D12.5 and ^{88}Y-Janus-2-(p-nitrobenzyl)-1,4,7,10-tetraazacyclododecane tetraacetic acid (DOTA) in BALB/c mice with KHJJ mouse adenocarcinoma: a model for ^{90}Y radioimmunotherapy. *Cancer Res* 1994;54:5937–5946.
19. Li M, Meares CF, Zhong G-R, Miers LA, Xiong C-Y, DeNardo SJ. Labeling monoclonal antibodies with ^{90}yttrium- and ^{111}indium-DOTA chelates: a simple and efficient method. *Bioconjug Chem* 1994;5:101–104.
20. Penefsky HS. A centrifuged-column procedure for the measurement of ligand binding by beef heart F1. *Methods Enzymol* 1979;56(part G):527–530.
21. Meares CF, McCall MJ, Reardan DT, Goodwin DA, Diamanti CI, McTigue M. Conjugation of antibodies with bifunctional chelating agents: isothiocyanate and bromoacetamide reagents, methods of analysis, and subsequent addition of metal ions. *Anal Biochem* 1984;142:68–78.
22. Beaumier PL, Neuzil D, Yang H-M, et al. Immunoreactivity assay for labeled anti-melanoma monoclonal antibodies. *J Nucl Med* 1986;27:824–828.
23. Adams GP, DeNardo SJ, Deshpande SV, et al. Effect of mass of ^{111}In-benzyl-EDTA-monoclonal antibody on hepatic uptake and processing in mice. *Cancer Res* 1989;49:1707–1711.
24. Coursey BM, Calhoun JM, Cessna JT. Radioassay of yttrium-90 used in nuclear medicine. *Nucl Med Biol* 1993;20:693–699.
25. Buchegger F, Rojas A, Delaloye AB, et al. Combined radioimmunotherapy and

radiotherapy of human colon carcinoma grafted in nude mice. *Cancer Res* 1995;55: 83–89.
26. Hosono M, Endo K, Hosono MN, et al. Treatment of small-cell lung cancer xenografts with iodine-131-anti-neural cell adhesion molecule monoclonal antibody and evaluation of absorbed dose in tissue. *J Nucl Med* 1994;35:296–300.
27. Wilder RB, McGann JK, Sutherland WR, et al. The hypoxic cytotoxin SR 4233 increases the effectiveness of radioimmunotherapy in mice with human non-Hodgkin's lymphoma xenografts. *Int J Radiat Oncol Biol Phys* 1993;28:119–126.
28. Govindarajulu, Z. *Statistical methods in bioassay.* New York: Karger; 1988:5–6.
29. Dulbecco R, Ginsberg HS. The nature of viruses. In: Davis BD, Dulbecco R, Eisen HN, Ginsberg HS, eds. *Microbiology*, 3rd Ed. Philadelphia: Harper and Row; 1980:883.
30. Berger MJ. Distribution of absorbed dose around point sources of electrons and beta particles in water and other media. *J Nucl Med* 1971;12(suppl 5):5–23.
31. Hui TE, Fisher DR, Kuhn JA, et al. A mouse model for calculating cross-organ beta doses from yttrium-90-labeled immunoconjugates. *Cancer* 1994;73(suppl):951–957.
32. Siegel JA, Wessels BW, Watson EE, et al. Bone marrow dosimetry and toxicity for radioimmunotherapy. *Antibodies Immunoconj Radiopharm* 1990;3:213–233.
33. DeNardo GL, Kukis DL, Shen S, et al. Efficacy and toxicity of ^{67}Cu-2IT-BAT-Lym-1 radioimmunoconjugate in mice implanted with human Burkitt's lymphoma (Raji). *Clin Cancer Res* 1997;3:71–79.
34. Siegel JA, Stabin MG. Absorbed fractions for electrons and beta particles in spheres of various sizes. *J Nucl Med* 1994;35:152–156.
35. Hollander M, Wolfe DA. *Nonparametric statistical methods.* New York: Wiley; 1973:120–123.
36. Agresti A. In: *Categorical data analysis.* New York: Wiley; 1990:283–287.
37. Casarett AP. Acute radiation effects in whole animals. In: Casarett AP, ed. *Radiation biology.* Edgewood Cliffs, NJ: Prentice-Hall; 1968:217–235.
38. Lewis JP, O'Grady LF, Green RA. Clinical and experimental: patterns of exogenous and endogenous hematopoietic repopulation following radiation injury. *J Lab Clin Med* 1977;89:229–239.
39. Thomas GE, Esteban JM, Raubitchek A, Wong JYC. Gamma-interferon administration after ^{90}yttrium radiolabeled antibody therapy: survival and hematopoietic toxicity studies. *Int J Radiat Oncol Biol Phys* 1995;31:529–534.
40. Schmidberger H, Buchsbaum DJ, Blazar BR, Everson P, Vallera DA. Radiotherapy in mice with yttrium-90-labeled anti-Ly1 monoclonal antibody: therapy of the T cell lymphoma EL4. *Cancer Res* 1991;51:1883–1890.
41. Marchese MJ, Zaider M, Hall EJ. Dose-rate effects in normal and malignant cells of human origin. *Br J Radiol* 1987;60:573–576.
42. Juweid M, Neumann R, Paik C, et al. Micropharmacology of monoclonal antibodies in solid tumors: direct experimental evidence for a binding site barrier. *Cancer Res* 1992;52:5144–5153.
43. Boucher Y, Baxter LT, Jain RK. Interstitial pressure gradients in tissue-isolated and subcutaneous tumors: implications for therapy. *Cancer Res* 1990;50:4478–4484.
44. Vaughan ATM, Anderson P, Dykes PW, Chapman CE, Bradwell AR. Limitations to the killing of tumors using radiolabelled antibodies. *Br J Radiol* 1987;60:567–578.
45. Langmuir VK, Fowler JF, Knox SJ, Wessels BW, Sutherland RM, Wong JY. Radiobiology of radiolabeled antibody therapy as applied to tumor dosimetry. *Med Phys* 1993;20(suppl 2):601–610.
46. Kuerbitz SJ, Plunkett BS, Walsh WV, Kastan MB. Wild-type p53 is a cell cycle checkpoint determinant following irradiation. *Proc Natl Acad Sci USA* 1992;89:7491–7495.
47. Lowe SW, Schmitt EM, Smith SW, Osborne BA, Jacks T. p53 is required for radiation-induced apoptosis in mouse thymocytes. *Nature* 1993;362:847–849.
48. Fan S, el-Deiry WS, Bae I, et al. p53 gene mutations are associated with decreased sensitivity of human lymphoma cells to DNA-damaging agents. *Cancer Res* 1994;54: 5824–5830.
49. Harris CC. Structure and function of the p53 tumor suppressor gene: clues for rational cancer therapeutic strategies. *J Natl Cancer Inst* 1996;88:1442–1455.
50. Gu Y, Sarnecki C, Aldape RA, Livingston DJ, Su MSS. Cleavage of poly(ADP-ribose) polymerase by interleukin-1B converting enzyme and its homologs TX and Nedd-2. *J Biol Chem* 1995;270:18715–18718.
51. Lane DP. Cancer. p53, guardian of the genome. *Nature* 1992;358:15–16.
52. Leek RD, Kaklamanis L, Pezzella F, Gatter KC, Harris AL. bcl-2 in normal human breast and carcinoma, association with oestrogen receptor-positive, epidermal growth factor receptor-negative tumours and in situ cancer. *Br J Cancer* 1994;69:135–139.

Technetium-99m-Sestamibi Scintimammography for the Detection of Breast Carcinoma: Comparison Between Planar and SPECT Imaging

Reinhold Tiling, Klaus Tatsch, Harald Sommer, Gabriele Meyer, Martina Pechmann, Katrin Gebauer, Wolfgang Münzing, Rainer Linke, Iraj Khalkhali and Klaus Hahn

Departments of Nuclear Medicine and Gynecology, Klinikum Innenstadt, Ludwig-Maximilians-University, Munich, Germany; and Department of Radiology, Division of Nuclear Medicine, Harbor-University of California, Los Angeles Medical Center, Torrance, California

The purpose of our study was to compare the results of planar and SPECT scintimammography for the detection of breast carcinoma. In addition, our goal was to determine whether SPECT reconstructed with filtered backprojection (FBP) or with iterative algorithms (ISA) can improve the sensitivity and specificity of planar scintimammography (SMM). **Methods:** One hundred thirteen patients with suspicious physical examinations and/or mammography underwent planar lateral and anterior breast imaging as well as SPECT imaging after injection of ^{99m}Tc-sestamibi. We used a blind evaluation, both separately and combined, for planar SMM, ISA-SPECT and FBP-SPECT. Scintigraphic findings were correlated with the final histopathological diagnoses. **Results:** The sensitivity of planar SMM was 80% with a specificity of 83%. All ISA-SPECT studies were of diagnostic quality, while FBP-SPECT was considered nondiagnostic in 14 that were excluded for statistical calculation. Sensitivity of ISA-SPECT and FBP-SPECT were 71% and 69%, respectively. Specificity was 70% for ISA-SPECT and 66% for FBP-SPECT. Combined planar SMM plus ISA-SPECT sensitivity was 85% (81% for planar SMM plus FBP-SPECT) with a specificity of 72%. Three carcinomas indeterminate on planar SMM were correctly identified by combined planar SMM plus ISA-SPECT. ISA-SPECT and FBP-SPECT provided additional information to planar SMM with respect to localization of sestamibi uptake, tumor extent, improved diagnostic certainty and detection of axillary nodes in 40 and 14 patients, respectively. **Conclusion:** ISA reconstruction is the preferable approach to SPECT data. Combined with planar SMM, ISA-SPECT can improve sensitivity. SPECT is useful in cases of indeterminate and positive planar SMM.

Key Words: scintimammography; SPECT; breast imaging; breast carcinoma

J Nucl Med 1998; 39:849–856

Carcinoma of the breast is the most common invasive malignancy in women and the second leading cause of cancer death among women in the U.S. (*1–3*). Since early breast cancer detection reduces mortality and allows breast-conserving surgical therapy, much work has been done to improve early breast cancer detection (*4*). The most succesful screening procedures are breast examinations and mammography, but both have

Received Feb. 1, 1997; revision accepted Aug. 6, 1997.

For correspondence or reprints contact: Reinhold Tiling, MD, Department of Nuclear Medicine, Ludwig-Maximilians-University of Munich, Marchioninistr. 15, 81377 Munich, Germany.